THE JOURNAL OF BIOLOGICAL CHEMISTRY VOL. 286, NO. 28, pp. 25246–25255, July 15, 2011

Phosphonoformic Acid Inhibits Viral Replication by Trapping the Closed Form of the DNA Polymerase*

Received for publication, April 7, 2011, and in revised form, May 6, 2011 Published, JBC Papers in Press, May 12, 2011, DOI 10.1074/jbc.M111.248864

Karl E. Zahn[‡], Egor P. Tchesnokov[§], Matthias Götte[§1], and Sylvie Doublié[‡2]

From the [‡]Department of Microbiology and Molecular Genetics, University of Vermont, Burlington, Vermont 05405 and the [§]Department of Microbiology and Immunology, McGill University, Montreal, Quebec H3A 2B4, Canada

Phosphonoformic acid (PFA, foscarnet) belongs to a class of antiviral drugs that inhibit the human cytomegalovirus DNA polymerase (UL54) by mimicking the pyrophosphate leaving group of the nucleotide transfer reaction. Difficulties expressing UL54 have hampered investigation of the precise structural requirements rendering inhibition by this drug. However, a previously engineered chimeric DNA polymerase, constructed by mutating the homologous polymerase from bacteriophage RB69 (gp43) to express several variable elements from UL54, can bypass this obstacle because of its favorable expression and acquired sensitivity to PFA (Tchesnokov, E. P., Obikhod, A., Schinazi, R. F., and Götte, M. (2008) *J. Biol. Chem.* 283, 34218–34228). Here, we compare two crystal structures that depict the chimeric DNA polymerase with and without PFA bound. PFA is visualized for the first time in the active site of a DNA polymerase, where interactions are resolved between the PP_i mimic and two basic residues absolutely conserved in the fingers domain of family B polymerases. PFA also chelates metal ion B, the cation that contacts the triphosphate tail of the incoming nucleotide. These DNA complexes utilize a primer-template pair enzymatically chain-terminated by incorporation of acyclo-GMP, the phosphorylated form of the anti-herpes drug acyclovir. We postulate that the V478W mutation present in the chimera is critical in that it pushes the fingers domain to more readily adopt the closed conformation whether or not the drug is bound. The closed state of the fingers domain traps the variant polymerase in the untranslocated state and increases affinity for PFA. This finding provides a model for the mechanism of UL54 stalling by PFA.

The human cytomegalovirus (HCMV)[3] belongs to the *herpesviridae* family, into which several important human pathogens are classified. A primary infection of this virus in pregnant mothers can be devastating to the developing fetus, resulting in several congenital disorders. Although a substantial portion of the global adult population is currently HCMV-seropositive, a functional immune system can hold the virus in check. For immunocompromised individuals, on the other hand, infection with HCMV presents a severe threat (1–3). Accordingly, antiviral therapy is used as both prophylaxis and therapeutic strategies in solid organ transplant recipients, who receive concomitant immunosuppressants. In this setting, infection with the virus is a major cause of morbidity and mortality.

The limited pharmacological options available for treatment of HCMV largely consist of nucleoside analog inhibitors that target the gene product of UL54, a family B DNA polymerase. Although some inhibitors, such as cidofovir, are chemically synthesized as acyclic nucleoside phosphonates, most nucleoside analogs require monophosphorylation by a viral kinase, such as UL97 in HCMV, before other cellular kinases convert these drugs into triphosphorylated substrates of the DNA polymerase (4). Following incorporation into the viral DNA, these non-natural nucleotides interfere with subsequent DNA synthesis by merit of either a distorted or absent 3′-hydroxyl (3′-OH) moiety. The nucleoside analog acyclovir, for example, becomes triphosphorylated to acyclo-GTP (Fig. 1), which contains both a guanine base and an acyclic sugar moiety lacking a 3′-OH that chain terminates DNA synthesis after incorporation at the primer terminus. Although acyclovir inhibits HCMV to a certain extent, this drug is not approved for treatment of HCMV (5). Rather, acyclovir serves primarily against herpes simplex viruses (HSVs), which are also members of *herpesviridae* and closely related to HCMV. Cidofovir and ganciclovir, on the other hand, provide approved treatment of HCMV, serving as nonobligate chain terminators that the polymerase extends poorly (6–8).

Phosphonoformic acid (PFA or foscarnet; Fig. 1) is a broad spectrum antiviral mimicking the pyrophosphate (PP_i) leaving group of the nucleotide transfer reaction. For the treatment of HCMV, PFA provides alternative inhibition of UL54 in second line regimens after accumulated resistance compromises nucleoside analog-based therapies. PFA additionally inhibits HIV-1 RT by trapping a DNA-bound pretranslocation complex, which suggests a common mechanism of action against other polymerases (9, 10). Many questions concerning the exact binding site of PFA have remained elusive, however, in part because poor expression levels of recombinant UL54 have precluded prior crystallographic investigation. Moreover, it is still unclear why PFA preferentially inhibits *herpesviridae* DNA

* This work was supported, in whole or in part, by National Institutes of Health Grant CA52040 (to S. D.). This work was also supported by a grant from the Canadian Institutes of Health Research (to M. G.). The beamline 23ID-B and the Advanced Photon Source were supported by National Cancer Institute Grant Y1-CO-1020, National Institute of General Medical Sciences Grant Y1-GM-1104, and U.S. Dept. of Energy, Basic Energy Sciences, Office of Science Contract DE-AC02-06CH11357.

[1] To whom correspondence may be addressed: McGill University, Dept. of Microbiology and Immunology, Duff Medical Bldg. (D-6), 3775 University St., Montreal, QC H3A 2B4. Tel.: 514-398-1365; Fax: 514-398-7052; E-mail: matthias.gotte@mcgill.ca.

[2] To whom correspondence may be addressed: Dept. of Microbiology and Molecular Genetics, The Markey Center for Molecular Genetics, University of Vermont, Stafford Hall, 95 Carrigan Dr., Burlington, VT 05405-0068. Tel.: 802-656-9531; Fax: 802-656-8749; E-mail: sdoublie@uvm.edu.

[3] The abbreviations used are: HCMV, human cytomegalovirus; PFA, phosphonoformic acid or foscarnet; 3′-OH, 3′ hydroxyl; TLS, translation, libration, and screw-rotation.

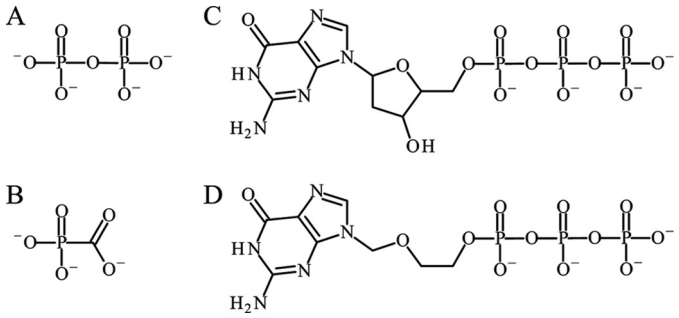

FIGURE 1. **Chemical structures of small molecules discussed in this manuscript.** *A*, PP_i. *B*, PFA (foscarnet). *C*, dGTP. *D*, acyclo-GTP. As is required of other nucleoside analog inhibitors, the viral thymidine kinases converts the nucleoside into the monophosphorylated form (acyclo-GMP), which is further phosphorylated into the active triphosphate (acyclo-GTP) by other cellular kinases.

polymerases, whereas other family B polymerases, such as RB69 DNA polymerase (gp43) or the replicative eukaryotic DNA polymerases δ or ϵ, are left unaffected by the drug (11).

The fingers domain in family B polymerases consists of two long helices, N and P, which contain two highly conserved basic protein residues (Arg-482 in helix N and Lys-560 in helix P) known to interact with the triphosphate tail of incoming nucleotides. Based on the hypothesis that the intervening variable regions between these conserved side chains might influence PFA inhibition in *herpesviridae*, a chimeric DNA polymerase, derived from the parental sequence of RB69 gp43, was engineered to express several of these variable elements originating from the fingers domain of UL54 (12). These elements consisted specifically of three blocks of amino acids adjacent to the absolutely conserved basic residues, Arg-482 and Lys-560 in gp43, therefore allowing the chimeric mutations considerable sequential proximity to the proposed PP_i binding site (see Fig. 4). Interestingly, these modifications transformed RB69 gp43 into a PFA-sensitive polymerase, without compromising high expression of the recombinant enzyme.

Here, we report the first crystal structure of any DNA polymerase-binding PFA. By comparing DNA complexes of the chimeric DNA polymerase with and without PFA bound, the exact structural requirements for PFA inhibition are unveiled. The primer termini in these structures are chain-terminated by acyclo-GMP, thus providing an added first glimpse of acyclovir in its fully metabolized active form at the primer terminus. We provide evidence that the sensitivity of the chimera to PFA arises primarily because of the V478W mutation, which induces a clash with helices of the N-terminal domain when the fingers open.

EXPERIMENTAL PROCEDURES

Nucleic Acids and Chemicals—Oligonucleotides for biochemical assays were purchased from Invitrogen. Primers were 5′-labeled with ^{32}P and gel-purified as described previously (13). Primer and template oligonucleotides for crystallization were synthesized by Midland Certified Reagent Company (Midland, TX) and gel-purified on 16% polyacrylamide denaturing gel, prior to desalting over Waters (Milford, MA) Sep-Pak C18 columns. New England Biolabs (Ipswich, MA) kindly provided acyclo-GTP, whereas deoxynucleotides were purchased from Fermentas Life Sciences. PFA was manufactured by Sigma-Aldrich, and PEG 20,000 stocks were purchased from Hampton Research (Aliso Viejo, CA). All other reagents were from either Sigma-Aldrich or Fisher and of the highest quality available.

Plasmid Constructs—The gp43 coding sequence was cloned into pPR-IBA1 (IBA) using the BsaI site to generate pPR-IBA1/gp43. This construct facilitates protein purification through Strep-tag affinity chromatography (IBA). The chimeric form of gp43 contains nine amino acid substitutions in helices N and P: V478W/F479V/N480S and I557M/N558A/R559L/L561V/L562T/I563C, respectively (see Fig. 4) (12). D222A and D327A substitutions were introduced to eliminate the 3′-5′ exonuclease activity of the polymerase for biochemical assays. The chimeric DNA polymerase used for crystallization only required mutation of one of the two catalytic aspartates (D222A), which also eliminates 3′-5′ exonuclease activity efficiently. Variant enzymes were generated by site-directed mutagenesis, utilizing PfuUltra DNA polymerase (Stratagene) to catalyze PCR according to the manufacturer's recommendations.

Protein Expression—The RB69 DNA polymerase wild-type, mutant, and chimeric enzymes were expressed as described previously, except from within the vector pPR-IBA1 (14). This expression plasmid encodes a C-terminal Strep-tag, which facilitated purification of all enzymes by affinity chromatography (IBA) according to the manufacturer's recommendations.

IC_{50} Experiments—IC_{50} experiments utilized the following templates: T1 = 5′-CCAATATTCACCATCAAGGCTTGACGTGACTTCACTCCACTATACCACTC and T2 = 5′-GGAAATCTCTAGCAGTGGCGCCCGAACAGGGACCTGAAAGCGAAAGGGAAAC. The underlined nucleotides are the portions of the templates that anneal to the primers, which were of the sequences: P1 (5′-GAGTGGTATAGTGGAGTGAA) and P2 (5′-GTTTCCCTTTCGCTTT).

The assay was conducted with 100 nM duplex DNA, obtained from annealing T1 to P1, and preincubated for 5–10 min at 37 °C with a given DNA polymerase in a buffer containing 25 mM Tris-HCl (pH 8), 50 mM NaCl, 0.5 mM DTT, 0.2 mg/ml bovine serum albumin, and 5% glycerol. To compare different enzymes in single nucleotide incorporation assays, we adjusted the enzyme concentration and the time point of the reaction such that ~40–50% of the primer substrate was used at the saturating concentration of dGTP (25 μM). Nucleotide incorporation was initiated by the addition of $MgCl_2$ to a final concentration of 10 mM, and the reactions were stopped by the addition of three reaction volumes of formamide containing traces of bromphenol blue and xylene cyanol. The samples were then subjected to 15% denaturing polyacrylamide gel electrophoresis, followed by phosphorimaging. The incorporation of single nucleotides was quantified as the fraction of the DNA substrate (primer *n*) converted to product (primer *n*+1). The extent of PFA-mediated inhibition of nucleotide incorporation was determined by plotting the percentage of dGMP incorporation against the concentration of PFA. IC_{50} values were calculated by fitting 11 data points to a sigmoidal dose response (variable slope) equation using GraphPad Prism (version 5.0). Standard deviations for all of the experiments were determined

on the basis of at least three independent replicates and represented a maximum of 20% of the reported IC_{50} value.

Crystallization—Oligonucleotides for crystallization consisted of the following sequences: P (5′-GCGGCTGTCATAA) and T (5′-CGTCTTATGACAGCCGCG), where the underlined portion of the template anneals to the primer, placing dCMP in templating position. The template 3′ end contains a dGMP that overhangs the primer and is required for essential crystal contacts between adjacent asymmetric units (15).

Chimeric RB69 DNA polymerase was dialyzed into a buffered solution containing 10 mM Hepes (pH 7.5), 50 mM NaCl, and 1 mM DTT and concentrated to 7 mg/ml. A reaction mixture for crystallization was then prepared by reacting 42 μM concentrated polymerase, 50 μM P/T, and 1 mM acyclo-GTP for 30 min at 25 °C. PFA (10 mM) and a crystallization buffer containing 10 mM Hepes (pH 7.5), 33 mM NaCl, 1 mM DTT, and 6 mM $MgCl_2$ were then added, bringing the final volume of reaction mixture to 12 μl. PFA was omitted for reactions intended to crystallize polymerase, P/T, and acyclo-GTP only.

An aliquot from 1 ml of reservoir solutions containing 3–5% (w/v) PEG 20 000, 100 mM ammonium acetate, 100 mM magnesium acetate, 100 mM Tris-HCl (pH 7.1–7.5), and 0.1% (v/v) glycerol was mixed with an equal volume of reaction mixture to create a 1-μl hanging drop. After 5–9 days of vapor equilibration at 25 °C, primitive orthorhombic crystals grew to a final size up to $100 \times 220 \times 40$ μm^3. These crystals were cryoprotected by adding 0.5 μl of a solution containing 7% (w/v) PEG 20,000 and 50% (v/v) glycerol directly to the hanging drop and plunged into liquid nitrogen.

Data Collection and Reduction—X-ray diffraction data were collected on a MAR m300 CCD detector at Beamline 23ID-B of the advanced photon source under cryocooled conditions (100 K). Measurements of intensity were integrated, scaled, and merged with version 1.98.4 of Denzo/Scalepack, yielding complete 2.7 Å data sets (see Table 1) (16). Merging observations from four crystals produced the high redundancy reported for the PFA complex. Although the R_{merge} is high, as can be expected from a data set with high redundancy, the $R_{Friedel}$ indicates that the data are of very high quality (17).

Isomorphous Replacement and Refinement—The structure without PFA was solved by isomorphous replacement using an RB69 ternary complex devoid of all nonprotein atoms as a starting model (Protein Data Bank code 2OZS) (18), after all nine amino acid side chains mutated in the chimeric enzyme were cropped to the β-carbon to avoid introduction of any model bias at these sites. Rigid body refinement was conducted with CNS on each protein domain, prior to subsequent TLS and residual B-factor refinement in Refmac (19, 20). The TLS model excluded both DNA and ligands and was based roughly on protein domains, where nonconsecutive regions of the same domain were further broken into unique TLS groups. $F_o - F_c$ maps revealed interpretable density for the chimeric mutations and duplex DNA, which unambiguously showed chain termination by acyclo-GMP. Chimeric side chains and DNA were built with the modeling software Coot (21). Because the chimeric RB69 polymerase does not contain the D327A mutation, a single metal ion was present in the exonuclease domain. The complete model was further refined by iterative rebuilding with Coot and refinement in Refmac.

The PFA complex was built using $F_o - F_o$ isomorphous difference maps generated with phases from the model lacking PFA, which was made possible by the high degree of isomorphism between the two crystal forms. The resulting electron density maps revealed without ambiguity that PFA was centered in the polymerase active site. Although several side chain rearrangements were indicated by peak-hole pairs, only minor rebuilding and refinement was needed to obtain the fully refined structure.

The refined B-factors in the deposited Protein Data Bank files represent residual B-factors. The B-factors indicated in Table 1 were averaged from anisotropic B-factors, derived from our refined TLS model by the software TLSANU and reported to avoid any unintentional misrepresentation of these values (22). Coordinates and structure factors were deposited into the Protein Data Bank under codes 3KD1 and 3KD5 for the complexes without and with PFA, respectively.

RESULTS

The Chimeric DNA Polymerase Crystallizes in the Closed Conformation with the DNA Untranslocated—The chimeric DNA polymerase complexed to a primer-template pair readily co-crystallized in both the presence and the absence of 10 mM PFA after the primer was chain-terminated by enzymatic incorporation of acyclo-GMP, yielding diffraction quality crystals able to scatter synchrotron radiation to 2.7 Å resolution. Unexpectedly, both of these crystal types indexed with primitive orthorhombic lattices and unit cell parameters characteristic of previous ternary complexes, even though the next complementary nucleotide following the acyclo-GMP was not present in these crystallization reactions. Subsequent isomorphous replacement verified this unanticipated result and showed that the fingers domain occupied the closed conformation typical of ternary complexes, regardless of the addition of PFA. The final models with and without PFA were refined to respective R_{free} values of 25 and 26%, while maintaining close geometric agreement with reference bond lengths and angles (Table 1).

Historically, capturing a closed ternary complex (enzyme, primer-template, and nucleotide) of any replicative DNA polymerase has required the presence of DNA lacking a functional 3′-OH, in addition to an incoming dNTP complementary to the templating nucleotide (15, 18, 23). Upon binding to the active site, the dNTP induces a conformational change, closing the fingers domain and trapping the complex at the enzymatic step directly preceding nucleophilic attack on the α-phosphate. A similar strategy utilizes a functional 3′-OH but requires a nonhydrolyzable nucleotide to stall the nucleotide transfer reaction (24). Although both structures of the chimeric DNA polymerase depict the closed conformation of the fingers domain, the untranslocated state of the DNA retains the 3′-incorporated acyclo-GMP at the insertion site (Fig. 2*A*), which distinguishes these models uniquely from previous structures. The complex without PFA is best described as a closed binary complex, to emphasize the closed configuration of the fingers domain in relation to conventional binary complexes that orient the fingers in the open conformation. The PFA complex is

TABLE 1
Crystallographic data collection and refinement statistics

	Acyclo-GMP, gp43-UL54 chimera	PFA, acyclo-GMP, gp43-UL54 chimera
Complex Type	Closed binary	Untranslocated ternary
Protein Data Bank code	3KD1	3KD5
Data collection		
Space group	$P2_12_12_1$	$P2_12_12_1$
Cell dimensions (*a*, *b*, *c*) (Å)	78.5, 121.7, 131.5	77.9, 122.4, 133.3
No. of crystals	1	4
Wavelength (Å)	1.03	1.03
Resolution (Å)	50-2.66 (2.76-2.66)[d]	40-2.70 (2.80-2.70)[d]
R_{merge} (%)[a]	10.6 (100)[d]	11.3 (100)[d]
$R_{Friedel}$ (%)[b]	7.2 (67.9)[d]	3.4 (44.6)[d]
$I/\sigma I$	17.7 (2.2)[d]	26.9 (3.4)[d]
Completeness (%)	100 (100)[d]	100 (100)[d]
Redundancy	7.6 (7.2)[d]	23.4 (21.1)[d]
No. of reflections	281,195 (36,963)[e]	843,202 (36,065)[e]
Refinement		
Resolution (Å)	30-2.66 (2.73-2.66)[d]	30-2.70 (2.76-2.7)[d]
No. of reflections	33291 (2672)[d]	32507 (2332)[d]
R_{work}/R_{free} (%)	20.8/24.8 (36.8/38.2)[d]	21.5/26.3 (34.7/38.0)[d]
No. of atoms	8349	8283
Protein	7379	7379
DNA (primer/template)	648 (284/364)	648 (284/364)
PFA molecule		7
Ions (Mg^{2+})	1	3
Water	321	246
Average B-factors (Å^2)[c]		
Protein	57.9	82.9
DNA (primer/template)	56.2 (61.3/52.2)	62.7 (64.8/61.1)
PFA molecule	NA	43.4
Ions (Mg^{2+})	71.8	47.8
Water	39.0	38.5
Root mean square deviations		
Bond lengths (Å)	0.006	0.006
Bond angles (°)	0.92	0.96

[a] $R_{merge} = \Sigma(|I_{hkl,i} - <I_{hkl}>|)/\Sigma(I_{hkl,i})$.
[b] $R_{Friedel} = \Sigma(|I_+ - I_-|)/\Sigma(<I>)$.
[c] Total B-factors reported were derived from residual isotropic B-factors with the program TLSANL (22), following TLS refinement. The TLS refinement model contained protein residues only.
[d] Highest resolution data are shown in parentheses.
[e] The total number of reflections is shown. The number of unique observations is shown in parentheses.

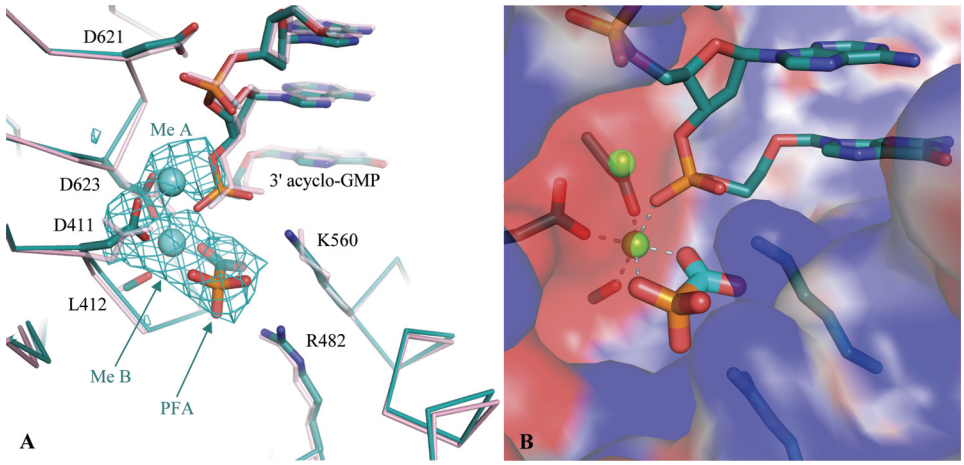

FIGURE 2. **Close-up view of the active site of the chimeric RB69 gp43.** *A*, a superposition of the ternary PFA complex (*cyan*) and the binary RB69 gp43-DNA complex (*pink*) is shown. The 2.7 Å $F_o - F_o$ map contoured at 3 σ reveals unbiased density for PFA, as well as metals A and B. Upon binding PFA, the conformation of the strictly conserved catalytic Asp-411 changes. The DNA has failed to translocate, which is indicated by the proximity of the incorporated acyclo-GMP to the catalytic aspartate residues (Asp-411 and Asp-623). *B*, the surface representation of the active site (*blue* for positive charges and *red* for negative charges) illustrates the multiple electrostatic interactions between PFA and the chimeric DNA polymerase.

conceptually similar to previously characterized closed ternary complexes, given that this new complex also shows a closed conformation and contains three different molecules—protein, DNA, and PFA—in the biological assembly. We expound the unique configuration of the DNA in the PFA structure by classifying it as an untranslocated, closed ternary complex. This liganded structure reflects the likely conformation of gp43 directly following phosphoryl transfer but prior to dissociation of PP_i, which is mimicked here by PFA.

The Active Site of the Closed Chimeric RB69 Polymerase Binds PFA—Difference Fourier methods were employed to compare diffraction data collected from isomorphous crystals

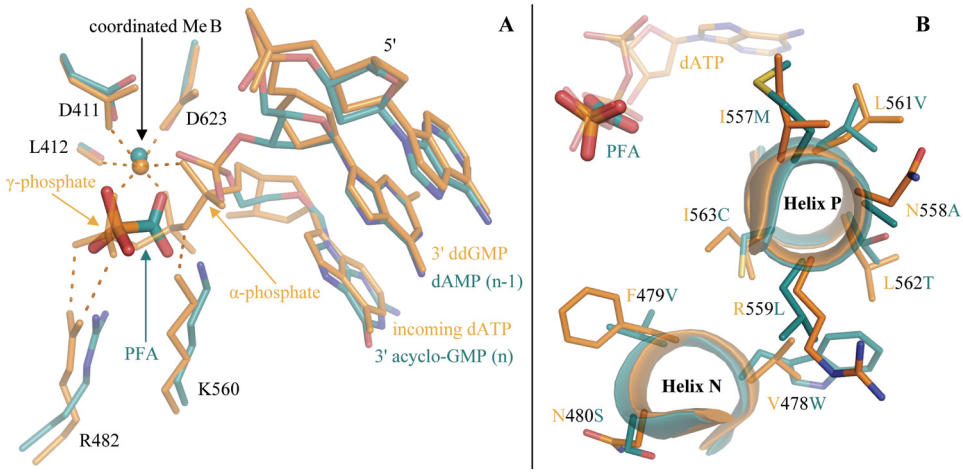

FIGURE 3. **Superpositions of the untranslocated, closed ternary complex of the chimeric DNA polymerase (*cyan*) with a translocated, closed ternary complex of RB69 gp43 (*orange*, Protein Data Bank code 2OZS) (18).** *A*, the PFA molecule overlaps with the β and γ phosphates of the incoming dATP, which is stabilized by conserved residues of the polymerase active site. *B*, no contacts are evident between the mutated residues and PFA, shown overlaid on the triphosphate tail of dATP (*top left*).

grown with and without PFA (25). The 2.7 Å $F_o - F_o$ electron density map presented a large positive peak centered in the polymerase active site, into which PFA was unambiguously modeled (Fig. 2*A*). The orientation of PFA suggests that the drug engages in electrostatic interactions with the two absolutely conserved basic residues of the fingers domain, Arg-482 and Lys-560 (Fig. 2*B*). By superimposing this structure with a previous translocated, closed ternary complex, we observed that the carboxyl group of PFA overlaps with the β-phosphate of an incoming dATP such that the phosphonate group mimics the γ-phosphate (Fig. 3*A*). Intriguingly, no other contacts to PFA were seen from any of the protein residues mutated to match the HCMV sequence (Fig. 3*B*). Together with the propensity of the chimeric DNA polymerase to crystallize with the fingers closed, these findings suggest that sensitivity to PFA is a function of polymerase conformation, rather than directed by specific side chain interactions unique to UL54.

PFA also interacts with the coordination sphere of metal ion B, contributing two contacts. Because PFA is known to chelate cations, this property appears essential for the capacity of the drug to mimic PP_i in the polymerase active site. Furthermore, metal ion A was resolved in the PFA structure, coordinated by single contacts from Asp-411 and Asp-623, in addition to two contacts from the backbone phosphate located 5′ of the primer terminus (Fig. 2*A*). The remaining two sites of the coordination sphere of this cation were filled by partially occupied water molecules. Metal ion A is not usually observed in translocated, closed ternary complexes of RB69 gp43 crystallized in the presence of Mg^{2+} because chain-terminated primers do not include a 3′-OH and therefore cannot complete the coordination requirements of the metal ion, unless a water molecule is able to satisfy this role (23). In the PFA complex, the O3′ of the $n - 1$ nucleotide in the untranslocated primer strand contacts metal ion A in a manner similar to that modeled for 3′-OH in translocated, closed ternary complexes of polymerase β captured with nonhydrolyzable nucleotide triphosphate analogs (24). This comparison suggests that the PFA complex represents the catalytic step directly following phosphoryl transfer, prior to dissociation of PP_i.

Unambiguous assignment of metal ions in polymerase structures is complicated because Mg^{2+} is devoid of anomalous signal and its atomic mass is such that its electron density cannot easily be distinguished from those of sodium cations or water molecules. Given that magnesium salts were present in both the crystallization reaction mixture and in the reservoir solution, we assigned the ions in the PFA complex as Mg^{2+}. The refined PFA structure exhibits an average coordination geometry of 2.2 Å over all 12 contacts, supporting that Mg^{2+} ions could occupy both the octahedral cation-binding sites (24). The use of calcium or manganese has resolved metal ion A in crystal structures of RB69 gp43 previously, although these ions are not expected to be physiological metals (15, 26). Calcium is coordinated at a greater distance than magnesium and inhibits DNA synthesis by distorting the active site. Manganese binds with higher affinity than magnesium and reduces the fidelity of DNA synthesis through relaxed coordination requirements (27, 28).

A Putative Clash between the N-terminal and Fingers Domains Favors the Closed Conformation—To identify roles for the chimeric protein residues in sensitizing gp43 to PFA, we compared previous unliganded structures of gp43 and HSV1 polymerase, a viral enzyme closely related to UL54 (15, 29). Without DNA, both polymerases crystallized with the fingers open, and the refined apo structures superimposed accordingly, with a root mean square deviation of 3.3 Å on C-α in core regions (30). This degree of fit was achieved with only 17% sequence identity and despite the presence of both an accessory domain at the N terminus of HSV1 polymerase and several loops conserved in *herpesviridae* that are not present in gp43. In fact, this lack of sequence homology would prohibit the alignment HSV1 polymerase and RB69 gp43 sequences in several key regions without the guidance of these apo structures. UL54, on the other hand, shares substantial sequence homology (31% identical) with HSV1 polymerase and an alignment based solely on sequence is readily generated (31). Because UL54 and HSV1 polymerase are so closely related, the structure-based alignment between HSV1 polymerase and RB69 gp43 can serve as an intermediate template, allowing for UL54 to be confidently

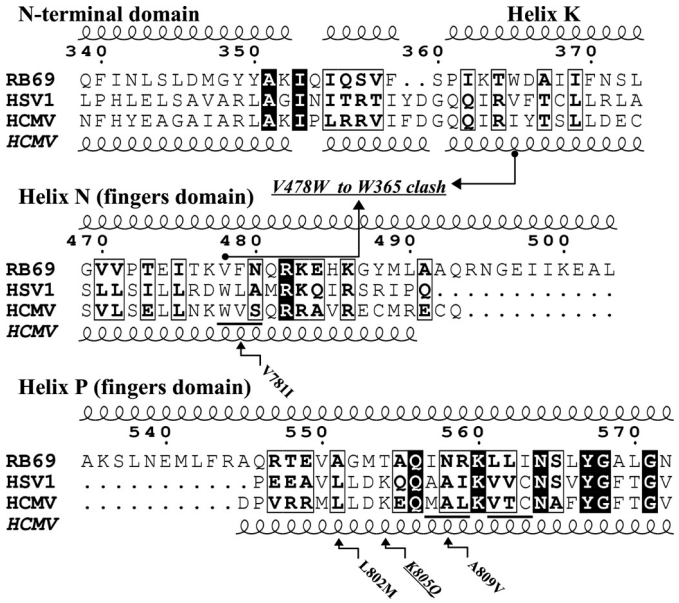

FIGURE 4. **Annotated sequence alignment (50) of family B polymerases from bacteriophage RB69, HSV1, and HCMV.** Residue numbers for RB69 are shown. The structure-based sequence alignment between RB69 and HSV1 is based on their apo structures (Protein Data Bank codes 1IH7 and 2GV9) (15, 29). Secondary structure elements depicted at the *top* correspond to RB69 gp43, whereas helices shown at the *bottom* are predicted for HCMV UL54 from the HSV1 structure. The three HCMV blocks *underlined* comprise the nine chimeric mutations introduced into RB69 gp43 to induce PFA sensitivity (12). The *arrows* linking amino acids 365 and 478 represent the clashing Trp residues in the chimeric DNA pol. The *small arrows* point out mutations known to arise in drug-resistant HCMV strains. The mutation K805Q marks a PFA-sensitizing mutation, unlike the others, which are associated with PFA resistance.

mapped onto gp43 in regions of marginal sequence conservation, such as in their N-terminal domains (Fig. 4).

The palm domains (residues 383–468 and 573–729) of the chimeric and apo gp43 polymerases superimpose on main chain atoms to a root mean square deviation of 0.6 Å. Because the fingers domain is closed in the chimeric polymerase and open in the apo gp43 model, this superposition effectively highlights the large pivoting motion that toggles the conformation of this domain, not only opening the active site as the fingers move away from the palm but also initiating closer contacts between helices N and P with the N-terminal domain. The apo HSV1 polymerase can be added to the superposition of chimeric and apo gp43 polymerases by aligning the conserved regions of the fingers domains of the two unliganded polymerases. Without any further modification, the resulting superposition provides an alignment of conserved elements in N-terminal domains of all three structures, such that the sites of the chimeric mutations in the fingers domain align well with the UL54-like sequence of apo HSV1 (Fig. 5).

A close inspection of the superposition of the chimeric DNA polymerase with apo RB69 gp43 and HSV1 polymerases reveals a putative clash from Trp-365, a residue present in helix K of the N-terminal domain, to the chimeric mutation V478W of the fingers domain (Fig. 5, *inset*) (32). Interestingly, RB69 gp43 is co-variant with *herpesviridae* polymerases at positions 365 and 478, where gp43 encodes Trp and Val, respectively. The opposite is true for *herpesviridae* polymerases, which encode a short hydrophobic residue in position 365 of the N-terminal domain and Trp in the fingers domain at residue 478. Ile represents the N-terminal residue present in the HCMV UL54 sequence (Fig. 4). Because the chimeric DNA polymerase harbors Trp residues both at sites 365 and 478, we hypothesized that a steric clash between these residues might hinder the open polymerase conformation, which would explain why the binary complex of the chimeric polymerase crystallized unexpectedly in the closed conformation.

The Chimeric V478W Mutation Alone Induces PFA Sensitivity in Parental RB69 gp43 exo—To test the contribution of V478W in inducing PFA sensitivity, we determined IC_{50} values for RB69 gp43 variants with and without the potential for a clash between Trp-478 and Trp-365 (Fig. 6). Reverting V478W to Val in the chimeric DNA polymerase increased the concentration of PFA required to achieve 50% inhibition of polymerase activity ~10-fold (Table 2). Conversely, the V478W mutation alone was able to sensitize the largely resistant parental RB69 gp43 exo- to an IC_{50} value of 6.3 μM PFA. To complement these data, we also generated mutants with amino acid changes in the N terminus. The W365V mutation, which removes the clashing Trp from the N-terminal domain, reverted PFA resistance in the chimera to levels higher than those measured for even the parental gp43. These findings provide strong evidence in support of our hypothesis that the crowding of amino acid side chains at the interface between the fingers and N-terminal domains effectively sensitizes RB69 gp43 to PFA.

DISCUSSION

The closed binary and ternary complexes of the chimeric DNA polymerase demonstrate the conformation of the fingers domain in polymerases experiencing inhibition by PFA. The drug binds exactly in the putative PP_i binding site, where the ability to concomitantly chelate metal ion B while engaging in active site electrostatics makes PFA well suited to stall the polymerase in the closed conformation. The ternary complex shows how the carboxylic acid of PFA is juxtaposed between Lys-560 and metal ion B. The phosphonate group at the other end of the molecule interacts with Arg-482, much like the γ-phosphate of an incoming nucleotide. Although PP_i departs rapidly from the polymerase active site as the natural byproduct of nucleotidyl transfer, the reduced charge present on PFA might slow its dissociation, especially if steric hindrance discouraged the transition to the open conformation, where Lys-560 and Arg-482 become too far from the active site to interact with either the primer terminus or the drug. Our mutational analysis of RB69 gp43 variants demonstrates that clashes between the N-terminal and fingers domains, which could hinder the open conformation, are key in the acquired PFA sensitivity of the chimeric DNA polymerase.

The untranslocated state of the DNA in complexes of the chimeric DNA polymerase distinguishes these structures as intermediates of the catalytic cycle not observed previously for replicative polymerases. Although wild-type gp43 prefers the open conformation in the DNA-bound ground state, the clashes present in the chimeric polymerase induce the closed binary complex. As a consequence of the fingers occupying the closed conformation, PFA binds in the retained PP_i-binding site when added to the crystallization mix, giving rise to the

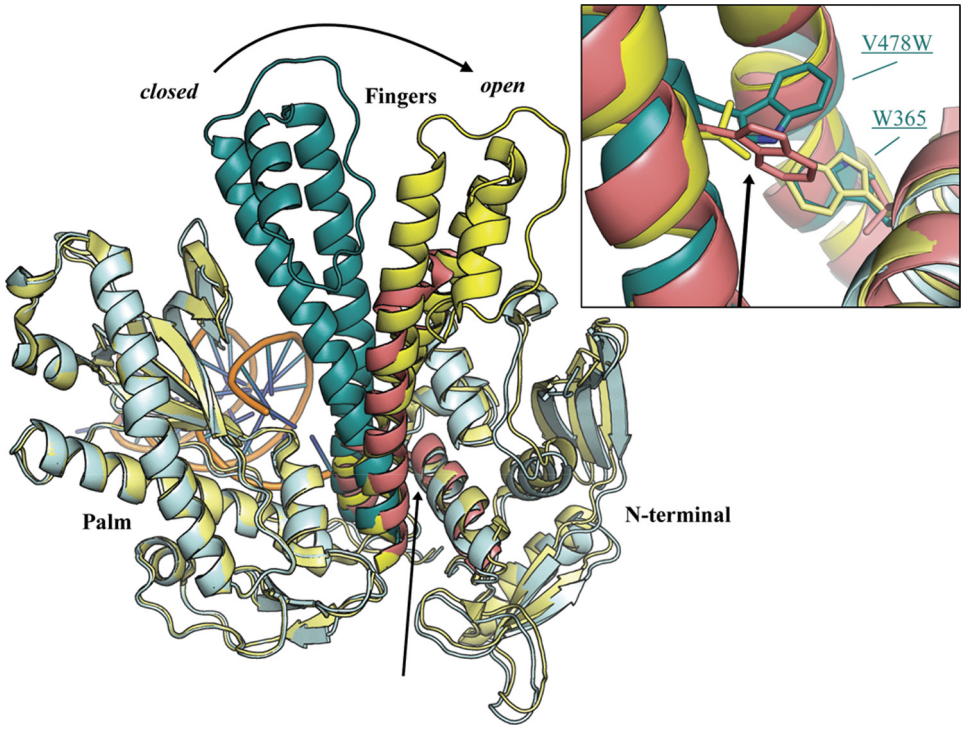

FIGURE 5. **Superposition of apo RB69 gp43 (*yellow*, Protein Data Bank code 1IH7) (15) and chimeric (*cyan*) DNA polymerase aligned on the palm domains (residues 383–468 and 573–729).** The conserved region of the fingers domain of apo HSV1 (*red*, Protein Data Bank code 2GV9) (29) was superimposed onto the corresponding segment of apo RB69 gp43, which produced good alignment of the N-terminal helices in all three structures. The *inset* provides a closer view of the putative clash, marked by *black arrows*, between V478W and Trp-365 in the chimeric DNA polymerase. For clarity, the thumb and exonuclease domains are omitted from this diagram.

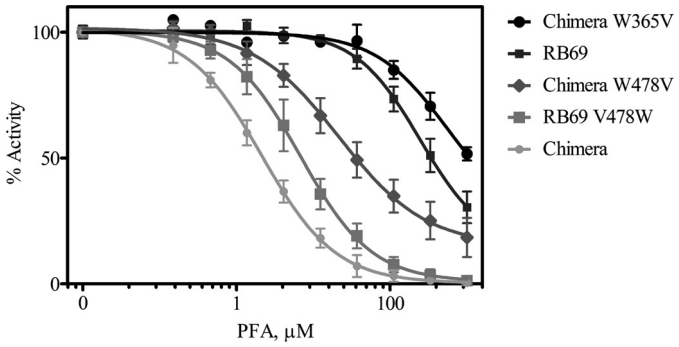

FIGURE 6. **PFA-mediated inhibition of single nucleotide incorporation events by variants of RB69 gp43 and the chimeric DNA polymerase.** *Darker shading* represents greater PFA resistance.

TABLE 2

IC_{50} values of RB69 DNA polymerase constructs

RB69 DNA polymerase construct	PFA IC_{50}[a]
	μM
RB69	>200
RB69_v478w	6.3
Chimera	2.1
Chimera_w365v	>200
Chimera_w478v	27

[a] Standard deviations were determined on the basis of at least three experiments and represent a maximum of 20% of the reported value.

untranslocated, closed ternary complex. Although our data cannot rule out the possibility that PFA could bind a post-translocation complex, the fact that the primer terminus provides key contacts to the coordination sphere of the metal ions suggests that the untranslocated state of the DNA is important for full affinity of the PFA molecule and its chelated metal.

The only currently available structures that compare with the PFA complex depict a *bona fide* PP_i in the active sites of Dpo4, stalled with a mismatched primer terminus, in addition to several mismatched or modified primer-template complexes of polymerase λ (27, 33). Although Dpo4 and polymerase λ are specialized for different biological roles, with Dpo4 sharing homology with family Y bypass polymerases and polymerase λ functioning in nucleotide gap repair as a member of family X, both Dpo4 and polymerase λ lack an appreciable conformational change during their respective catalytic cycles, which implies the preformed nature of their active sites (34). In the case of the chimeric DNA polymerase, an active site mismatch was not required to stall translocation of the DNA and obtain the PFA complex. The chimeric mutations minimally perturb the closed polymerase conformation (Fig. 3*B*), and for this reason, the PFA complex structure likely mirrors transient stalling of the viral polymerase caused by the mode of action of this drug. This observation infers that the characteristic PFA sensitivity in *herpesviridae* polymerases is a consequence of the conformational equilibrium of the fingers domain being biased toward the closed state, compared with RB69 gp43. By impinging on this equilibrium, the clashing Trp residues in the chimeric RB69 DNA polymerase therefore provide a synthetic means of modeling the PFA inhibition complex.

Motif A Interacts with PFA and Appears Implicated in the Conformational Change—Motif A represents a hallmark feature of the palm domain of family B polymerases, which universally encode the amino acid residues D*XX*SLYPS (residues Asp-411 to Ser-418 of RB69 gp43) in conserved region II (35–37). For some time, a mutation in this motif that substitutes the Leu

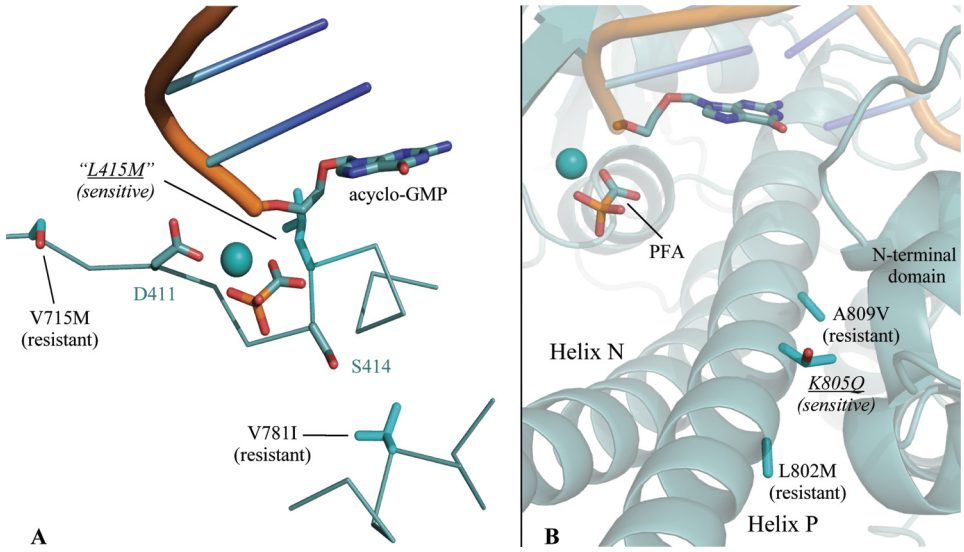

FIGURE 7. **The positions of mutations modifying PFA sensitivity in UL54 (*black font*) are mapped onto the chimeric DNA polymerase (*cyan font*) in complex with PFA.** *A*, mutations altering PFA-binding span motif A (D*XX*SLYPS). *B*, clinically relevant mutations of the fingers domain from HCMV UL54 present side chains on the N-terminal side of helix P, close to secondary structure elements of the N-terminal domain.

(Leu-415 in RB69 gp43) with Met has been known to sensitize T4 DNA polymerase (T4 gp43) to inhibition by PFA, which was discovered by screening for suppression of restrictive T4 growth on the *optA1* host (38). *optA1* starves phage for dGTP, and the L415M mutation is believed to stabilize the replicating complex at the expense of the exonuclease proofreading mode. This repartitioning of catalytic activities enables L415M-like variants to bind more tightly to dGTP and proliferate in the restrictive *optA1* environment (39). In our crystal structures, the backbone amino group of Leu-415 is poised very close to the PP_i-binding pocket, although the side chain of this residue points away from the active site and does not interact with PFA. This orientation places the acidic end of the PFA molecule in close contact with the Leu-415 amide, which are separated by less than 3.5 Å (Fig. 7*A*). Furthermore, the orientation of the Leu-415 side chain, which is directed away from the fingers and into the palm, makes it unlikely that the L415M mutation would cause an interdomain steric clash. For this reason, it appears likely that the PFA sensitivity of L415M variants might arise because of a distinct mechanism.

The single substantial difference between protein residues observed in the chimeric DNA polymerase crystallized with and without PFA appeared at Asp-411 of motif A. Upon binding PFA, the side chain of Asp-411 moves, bringing the carboxylates into contact with metal ions A and B (Fig. 2*A*). Apparently, the closed fingers and untranslocated DNA do not dictate the configuration of Asp-411, whose conformational freedom is demonstrated by comparing these complexes. Although not as dramatic as the closure of the fingers domain, this rearrangement in Asp-411 appears as an additional requirement for PFA binding. In contrast, the second catalytic Asp (Asp-623), conserved in the DTDS motif of region I, is buried deeper into the palm and does not move upon PFA binding. Given the sequence proximity of Asp-411 to Leu-415, the conformational freedom at Asp-411 might be affected by the L415M mutation, which could increase the occupancy of this catalytic residue toward the PFA-binding conformation through small adjustments in the protein backbone of motif A.

Implications for HCMV-resistant Strains—We have hypothesized that PFA sensitivity is imposed by at least two different mechanisms associated with stabilization of the replicating complex: 1) mutations in motif A discourage dissociation of PFA (and potentially PP_i or nucleotides) from the polymerase active site by interfering with small conformational changes at Asp-411 or 2) steric clash between the fingers and N-terminal domains favors the closed conformation and thereby increases the binding affinity for the drug. Although many mutations sequenced from resistant HCMV isolates map to divergent regions of the UL54 gene, clustering is evident in both conserved region II of the palm domain, adjacent to motif A, and in the fingers domain, especially coincident with region III, which overlaps with a portion of helix P (Fig. 4) (40, 41). A similar distribution of resistance mutation has been identified in HSV1 clinical isolates, further supporting an important role for polymerase regions II and III in acquired PFA resistance (42).

The UL54 mutations T700A and V715M of region II correspond to palm residue positions Phe-395 and Ser-409 in RB69 gp43, respectively, and have been confirmed as enhancers of PFA resistance in recombinant UL54 (43). Although the specific mutation T700A is not included in the protein regions that we have discussed in detail, the main chain atoms in the vicinity of this residue make van der Waals contact with the minor groove of the template DNA strand, as can be observed at residue Phe-395 in RB69 gp43 crystal structures. The T700A mutation could therefore loosen the grasp of the polymerase on the DNA, thereby enhancing diffusion of DNA and PFA away from the enzyme. On the other hand, the V715M mutation in UL54 lies adjacent to the catalytic aspartate of motif A (Asp-411 in RB69 gp43 and Asp-717 in HCMV UL54) (Fig. 7*A*). In RB69 gp43, this mutation maps to Ser-409, which leaves one residue between the position of the mutation and Asp-411, the aspartate that undergoes a conformational shift upon PFA binding.

The local secondary structure involving these residues forms a β-strand of the palm, and the side chains therefore lie in close proximity, potentially allowing the V715M mutation to hinder the necessary conformational changes in motif A for tight binding of PFA. Together with the sensitivity of the L415M gp43 variants, this resistance in V715M UL54 makes evident mutations spanning motif A that yield both positive and negative modulation of PFA resistance.

A substantial fraction of residue substitutions involved in UL54-mediated PFA resistance has been found in the fingers domain. The HCMV V781I mutation maps within the first mutant block of the chimeric DNA polymerase, at the position of F479V one turn of helix N away from Arg-482 (44). The side chain of this residue faces the palm domain and resides close enough to the second serine in motif A that V781I would be predicted to enter into van der Waals contact with these highly conserved residues when the fingers close (Fig. 7*A*). V781I might therefore function in the same pathway as V715M, which we suggested impedes tight binding of PFA by hindering movement of Asp-411. It is also possible, however, that a mutation in helix N facing the palm could clash such that the closed complex was sterically hindered, although a severe disruption of the replicating complex would be expected to inactivate the enzyme.

Helix P spans the majority of conserved region III, which contains many residues found in PFA resistant HCMV. Effectors of resistance are L802M, K805Q, A809V, T821I, and A834P, where all mutations induce resistance in UL54 except for K805Q, which is known to bring about sensitivity and was isolated from cidofovir-resistant strains (44–48). Interestingly, our alignments propose that the mutations L802M, K805Q, and A809V span a helical section that overlaps with the first block of chimeric mutations (Fig. 7*B*). The spacing of three or four residues is not a likely coincidence, because this interval positions all of these side chains on the back of helix P where they face the N-terminal domain, much like the clashing chimeric mutation V478W of helix N (Fig. 5) (49). Further pooling these mutations with the residue substitutions of the chimeric DNA polymerase reveals a trend where adding hydrophobic surface (L802M or A809V) could possibly stabilize the open form of the polymerase, favoring interaction with hydrophobic surface of the N-terminal domain, whereas clashing or hydrophilic substitutions (V478W or K805Q) seem to enhance sensitivity and favor the closed conformation, where the back of the fingers domain remains solvent-exposed.

Conclusion—Our crystallographic analysis of the chimeric RB69 gp43 establishes that PFA inhibits HCMV UL54 by trapping the closed, untranslocated form of the polymerase complexed to DNA. While chelating metal ion B, PFA binds to evolutionarily conserved basic residues of the fingers domain required for the efficient catalysis of phosphoryl transfer. Because the polymerase establishes similar electrostatic contacts with both PFA and the tails of incoming dNTPs, selection for resistance drives mutations at other sites. Some of these mutable sites seem to impinge on motif A of the palm domain. Others appear in regions of the polymerase interacting with the DNA, perhaps suggesting that the concomitant release of the DNA provides a pathway for escaping the electrostatic interactions evident in the PFA stalled complex. Our mutational analysis of RB69 gp43 has shown that a clash biasing the polymerase toward the closed conformation drives PFA sensitivity in the chimeric DNA polymerase, and this artifact was key in allowing us to model PFA binding in the polymerase active site. With a conformational equilibrium skewed toward the closed form, the RB69 gp43 chimera variant therefore provides a route for analysis of transient intermediates not otherwise observable in replicative DNA polymerases and could serve as a scaffold for future drug design aimed to stall UL54 in the untranslocated, closed form.

REFERENCES

1. Mercorelli, B., Sinigalia, E., Loregian, A., and Palù, G. (2008) *Rev. Med. Virol.* **18,** 177–210
2. Abou-Zeid, K. A., Yoon, K. S., Oscar, T. P., Schwarz, J. G., Hashem, F. M., and Whiting, R. C. (2007) *J. Food Prot.* **70,** 2620–2625
3. Lerner, C. W., and Tapper, M. L. (1984) *Medicine* **63,** 155–164
4. De Clercq, E., and Holý, A. (2005) *Nat. Rev. Drug Discov.* **4,** 928–940
5. Spector, S. A., and Kelley, E. (1985) *Antimicrob. Agents Chemother.* **27,** 600–604
6. Magee, W. C., Aldern, K. A., Hostetler, K. Y., and Evans, D. H. (2008) *Antimicrob. Agents Chemother.* **52,** 586–597
7. Reardon, J. E. (1989) *J. Biol. Chem.* **264,** 19039–19044
8. Tchesnokov, E. P., Obikhod, A., Schinazi, R. F., and Götte, M. (2008) *J. Biol. Chem.* **283,** 34218–34228
9. Marchand, B., Tchesnokov, E. P., and Götte, M. (2007) *J. Biol. Chem.* **282,** 3337–3346
10. Beilhartz, G. L., Wendeler, M., Baichoo, N., Rausch, J., Le Grice, S., and Götte, M. (2009) *J. Mol. Biol.* **388,** 462–474
11. Li, L., Murphy, K. M., Kanevets, U., and Reha-Krantz, L. J. (2005) *Genetics* **170,** 569–580
12. Tchesnokov, E. P., Obikhod, A., Schinazi, R. F., and Götte, M. (2009) *J. Biol. Chem.* **284,** 26439–26446
13. Tchesnokov, E. P., Gilbert, C., Boivin, G., and Götte, M. (2006) *J. Virol.* **80,** 1440–1450
14. Hogg, M., Wallace, S. S., and Doublié, S. (2004) *EMBO. J.* **23,** 1483–1493
15. Franklin, M. C., Wang, J., and Steitz, T. A. (2001) *Cell* **105,** 657–667
16. Otwinowski, Z., and Minor, W. (1997) *Methods Enzymol.* **276,** 307–325
17. Rould, M. A. (1997) *Methods Enzymol.* **276,** 461–472
18. Zahn, K. E., Belrhali, H., Wallace, S. S., and Doublié, S. (2007) *Biochemistry* **46,** 10551–10561
19. Brunger, A. T. (2007) *Nat. Protoc.* **2,** 2728–2733
20. Winn, M. D., Murshudov, G. N., and Papiz, M. Z. (2003) *Methods Enzymol.* **374,** 300–321
21. Emsley, P., and Cowtan, K. (2004) *Acta Crystallogr. D Biol. Crystallogr.* **60,** 2126–2132
22. Howlin, B., Butler, S., Moss, D., Harris, G., and Driessen, H. (1993) *J. Appl. Crystallogr.* **26,** 622–624
23. Doublié, S., Tabor, S., Long, A. M., Richardson, C. C., and Ellenberger, T. (1998) *Nature* **391,** 251–258
24. Batra, V. K., Beard, W. A., Shock, D. D., Krahn, J. M., Pedersen, L. C., and Wilson, S. H. (2006) *Structure* **14,** 757–766
25. Stein, M., Spencer, D., Kantor, A., Lakier, R., Lachter, J., Ben-Yosef, R., and Bezwoda, W. R. (1994) *Tumori* **80,** 216–219
26. Hogg, M., Rudnicki, J., Midkiff, J., Reha-Krantz, L., Doublié, S., and Wallace, S. S. (2010) *Biochemistry* **49,** 2317–2325
27. Garcia-Diaz, M., Bebenek, K., Krahn, J. M., Pedersen, L. C., and Kunkel, T. A. (2007) *DNA Repair* **6,** 1333–1340
28. Zakharova, E., Wang, J., and Konigsberg, W. (2004) *Biochemistry* **43,** 6587–6595
29. Liu, S., Knafels, J. D., Chang, J. S., Waszak, G. A., Baldwin, E. T., Deibel, M. R., Jr., Thomsen, D. R., Homa, F. L., Wells, P. A., Tory, M. C., Poorman, R. A., Gao, H., Qiu, X., and Seddon, A. P. (2006) *J. Biol. Chem.* **281,** 18193–18200
30. Krissinel, E., and Henrick, K. (2004) *Acta Crystallogr. D Biol. Crystallogr.*

60, 2256–2268
31. Edgar, R. C. (2004) *Nucleic Acids Res.* **32,** 1792–1797
32. Wang, J., Sattar, A. K., Wang, C. C., Karam, J. D., Konigsberg, W. H., and Steitz, T. A. (1997) *Cell* **89,** 1087–1099
33. Vaisman, A., Ling, H., Woodgate, R., and Yang, W. (2005) *EMBO. J.* **24,** 2957–2967
34. Xu, C., Maxwell, B. A., Brown, J. A., Zhang, L., and Suo, Z. (2009) *PLoS Biol*. **7,** e1000225
35. Wong, S. W., Wahl, A. F., Yuan, P. M., Arai, N., Pearson, B. E., Arai, K., Korn, D., Hunkapiller, M. W., and Wang, T. S. (1988) *EMBO. J.* **7,** 37–47
36. Ito, J., and Braithwaite, D. K. (1991) *Nucleic Acids Res.* **19,** 4045–4057
37. Delarue, M., Poch, O., Tordo, N., Moras, D., and Argos, P. (1990) *Protein Eng.* **3,** 461–467
38. Reha-Krantz, L. J., Nonay, R. L., and Stocki, S. (1993) *J. Virol.* **67,** 60–66
39. Reha-Krantz, L. J., and Nonay, R. L. (1994) *J. Biol. Chem.* **269,** 5635–5643
40. Baldanti, F., and Gerna, G. (2003) *J. Antimicrob. Chemother*. **52,** 324–330
41. Baldanti, F., Lurain, N., and Gerna, G. (2004) *Hum. Immunol*. **65,** 403–409
42. Gilbert, C., Bestman-Smith, J., and Boivin, G. (2002) *Drug Resist. Updat*. **5,** 88–114
43. Baldanti, F., Underwood, M. R., Stanat, S. C., Biron, K. K., Chou, S., Sarasini, A., Silini, E., and Gerna, G. (1996) *J. Virol.* **70,** 1390–1395
44. Smith, I. L., Cherrington, J. M., Jiles, R. E., Fuller, M. D., Freeman, W. R., and Spector, S. A. (1997) *J. Infect. Dis.* **176,** 69–77
45. Chou, S., Marousek, G., Guentzel, S., Follansbee, S. E., Poscher, M. E., Lalezari, J. P., Miner, R. C., and Drew, W. L. (1997) *J. Infect. Dis.* **176,** 786–789
46. Cihlar, T., Fuller, M. D., and Cherrington, J. M. (1998) *J. Virol.* **72,** 5927–5936
47. Chou, S., Marousek, G., Parenti, D. M., Gordon, S. M., LaVoy, A. G., Ross, J. G., Miner, R. C., and Drew, W. L. (1998) *J. Infect. Dis.* **178,** 526–530
48. Scott, G. M., Weinberg, A., Rawlinson, W. D., and Chou, S. (2007) *Antimicrob. Agents Chemother.* **51,** 89–94
49. Shi, R., Azzi, A., Gilbert, C., Boivin, G., and Lin, S. X. (2006) *Proteins* **64,** 301–307
50. Gouet, P., Courcelle, E., Stuart, D. I., and Métoz, F. (1999) *Bioinformatics* **15,** 305–308